ELSEVIER

Polymer 42 (2001) 1319–1327

polymer

www.elsevier.nl/locate/polymer

Polycyclic silicone membranes. Synthesis, characterization and permeability evaluation

S.U.A. Redondo[a], E. Radovanovic[a], I.L. Torriani[b], I.V.P. Yoshida[a,*]

[a]*Instituto de Química, Universidade de Campinas, CP 6154, 13083-970, Campinas, São Paulo, Brazil*
[b]*Instituto de Física, Universidade de Campinas, CP 6154, 13083-970, Campinas, São Paulo, Brazil*

Received 13 January 2000; accepted 5 July 2000

Abstract

In this work, membranes based on polycyclic silicone networks were synthesized from different cyclic siloxanes, through hydrosilylation reactions. These membranes showed good thermal stability, glass transition higher than conventional silicone networks and the absence of pores and phase segregation, with roughness surface. The nanomorphology of the materials was studied by small angle X-ray scattering. Some samples produced practically no scattering and some produced patterns that are typical of non-particulate systems. The gas permeability behavior of the membranes was investigated, showing permeability coefficients higher than those observed for some organic polymers, and selectivity coefficients higher than those found for PDMS based membranes.

Keywords: Cyclosiloxanes; Hydrosilylation; Membranes

1. Introduction

Among semi-inorganic polymers, polysiloxanes or silicones are by far the most studied, especially the widely used commercial poly(dimethylsiloxane) (PDMS). The presence of methyl groups attached to a backbone of Si–O–Si bonds gives to PDMS a combination of unique properties, such as excellent thermal and oxidative stabilities, biological and chemical inertness, low surface tension and high gas permeability [1].

Siloxane polymers are also well known due to their highly flexible backbone, which gives to PDMS one of the lowest glass transition temperatures (T_g) of −127°C [2]. The dynamic flexibility of PDMS can be explained by the low rotation barriers about the Si–O bonds, associated to the presence of an unsubstituted small atom (oxigen) between the substituted silicon atoms, and also to a Si–O bond 1.64 Å longer than a C–C bond 1.53 Å [1–3].

It has been demostrated that the purely thermal degradation of linear PDMS results in chain depolymerization, and that $-(CH_3)_2SiOH$ terminated PDMS is less thermally stable than $(CH_3)_3Si-$ end-blocked polymers [4–6]. The mechanism of degradation is based on the intermolecular and intramolecular interchange reactions, whose major products are cyclic compounds D_3 and D_4 [7].

The thermal stability of the silicones can be improved by the insertion of rigid groups into the chain backbone, such as phenylene in poly(silphenylenesiloxane), where the rigid structures decrease the intrachain rearrangements [8]. Another way to improve the thermal stability is through polymer network formation. In polymer networks, the usual degradation mechanisms are minimized, due to higher restriction of the rearrangements, and to suppression of reactive endblocks [9].

Another important feature of siloxane polymers is their unusually high gas permeability. The presence of high free volume compared to hydrocarbons explains the high solubility and high diffusion coefficient of gases [10]. The growing importance of PDMS and other silicone polymers as gas separation membranes, in particular for the oxygen enrichment of air, has been evident in spite of their low selectivities [11]. In the last years, several studies varying the basic siloxane structure to improve the selectivity without decreasing the permeability of the membranes, were described [10].

In this work, vinyl and hydrogen functionalized cyclic siloxanes, such as 1,3,5,7-tetravinyl,1,3,5,7-tetramethylcyclotetrasiloxane and 1,3,5,7-tetramethylcyclotetrasiloxane were used as basic units, together with different kinds of molecules containing Si–H or $Si–CH=CH_2$ groups, in the

* Corresponding author. Tel.: +55-19-788-2121; fax: +55-19-7883023.
E-mail address: valeria@iqm.unicamp.br (I.V.P. Yoshida).

0032-3861/01/$ - see front matter
PII: S0032-3861(00)00520-6

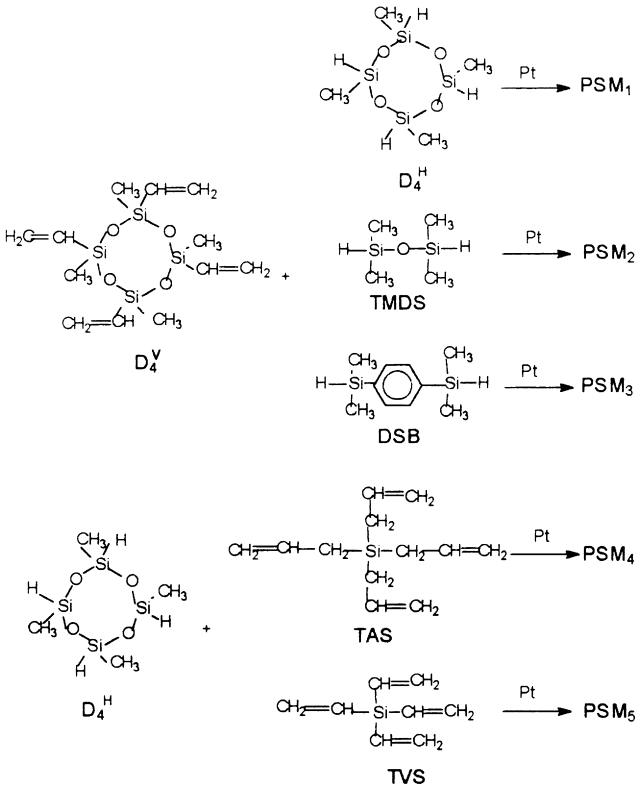

Fig. 1. Reaction schemes for the preparation of polycyclic silicone membranes.

formation of polymeric networks, through hydrosilylation reactions. These materials were characterized and their gas permeabilities were evaluated.

2. Experimental

2.1. Materials

Commercially available cyclic siloxanes 1,3,5,7-tetravinyl,1,3,5,7-tetramethylcyclotetrasiloxane (D_4^V) and 1,3,5,7-tetramethylcyclotetrasiloxane (D_4^H) were supplied by Dow Corning. The platinum–divinyltetramethyldisiloxane complex (Pt catalyst, 3–3.5% platinum concentration in vinyl terminated poly(dimethylsiloxane)) was supplied by Gelest. The monomers 1,1′,3,3′-tetramethyldisiloxane (TMDS) and tetravinylsilane (TVS), purchased from Aldrich Chemical Corporation, were used as received. The monomers 1,4-bis(dimethylsilyl)benzene (DSB) and tetraallylsilane (TAS) were synthesized according to Pittman et al. [12] and O'Brien et al. [13] procedures, respectively, and were purified and characterized before use.

2.2. Sample preparation

In this study, five different polycyclic silicone membranes (PSM), as self-supported films, were prepared by means of hydrosilylation reaction from mixtures of D_4^V and D_4^H; D_4^V and TMDS; D_4^V and DSB; D_4^H and TAS, and finally D_4^H and TVS, giving rise to samples that will be referred to as: PSM_1, PSM_2, PSM_3, PSM_4 and PSM_5, respectively, as can be seen in Fig. 1.

The PSM_1, PSM_2 and PSM_3 membranes were obtained in the absence of solvent, by mixing the vinylsiloxane and Pt catalyst (1% in relation to total mass) for 15 min, followed by the addition of hydridesilane and homogenized under magnetic stirring for more 15 min. The mixtures were cast onto Teflon® Petri dishes and let stand at room temperature for 72 h. The samples were then submitted to an isothermal treatment at 70°C, in a vacuum oven, for 16 h. The PSM_4 and PSM_5 samples were obtained in the presence of toluene as solvent, following the same procedure described above. All these reactions were carried out with Si–H : $SiCH{=}CH_2$ 1:1 molar ratio.

2.3. Methods

2.3.1. Nuclear magnetic resonance and Raman spectra

Solid-state ^{29}Si nuclear magnetic resonance spectra (^{29}Si MAS NMR) were performed on a Bruker AC300 spectrometer at a 59.6 MHz resonance frequency, applying magic angle spinning (MAS) technique, with 10 min delay time between 90° pulses. Raman spectra were obtained by means of a FT-Raman, Bomen DA8 spectrometer, using the 1604-nm radiation from Nd:YAG laser excitation, in the spectral range 400–3000 cm^{-1} at a 4 cm^{-1} resolution.

2.3.2. Thermogravimetric analysis (TGA)

Thermogravimetric analysis of PSM membranes were carried out in a TA 2950 thermobalance, TA Instruments, in the range of 25–1000°C, at a scanning rate of 20°C/min, under argon flow.

2.3.3. Dynamic mechanical analysis (DMA)

The dynamic mechanical behavior of these materials was analyzed using a TA Instrument DMA 983, in a tension mode, fixed frequency (1 Hz), in the range of −150 to 200°C, at a scanning rate of 5°C/min. The maximum in the curve of log E'' as a function of temperature, was defined as T_g.

2.3.4. Morphological analyses

The morphology of the polycyclic silicones was analyzed by field emission scanning electron microscopy (FESEM) using a JM-6340F, JEOL microscope, operated at 5 kV. The surface observed was obtained by coating a cryogenic fracture with a thin gold layer.

The images of the surface membranes were obtained using atomic force microscopy (AFM) on a Discoverer TMX 2000 instrument, Topometrix, by non-contact mode technique, with a Nanoprobe of 70 μm length, and a high resonance frequency (HRF) pyramidal silicon cantilever with a spring constant of 35 N m^{-1}, model 1650-00,

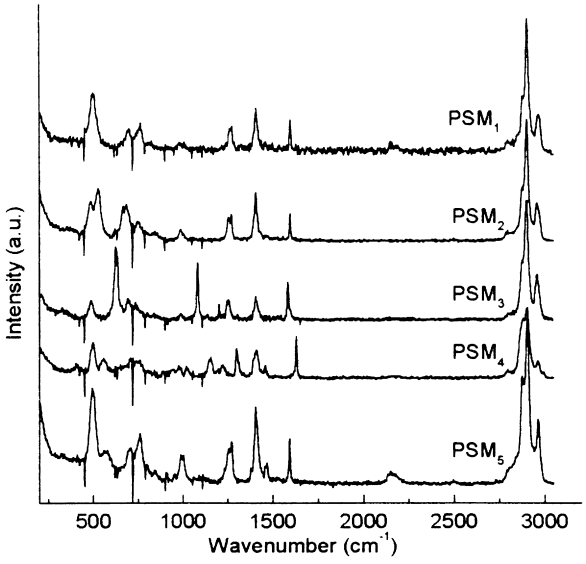

Fig. 2. Raman spectra of polycyclic silicone membranes.

Topometrix. The images were processed only by flattening to remove background slope.

2.3.5. Small angle X-ray scattering (SAXS)

The small angle X-ray scattering measurements were performed at the SAXS workstation of the National Synchrotron Light Laboratory, LNLS, Campinas-SP, Brazil. In this workstation, the X-ray beam is horizontally focused and monochromatized by a curved (111) silicon crystal ($\lambda = 1.608$ Å), the beam was defined by two sets of slits. The measurements were taken at room temperature under vacuum. The SAXS intensity functions $I(q)$ were registered using linear position sensitive detector. Parasitic scattering was subtracted from the total intensity. Corrections for sample absorption and detector response were also introduced. Scattering curves were recorded at a sample–detector distance of 1282.5 mm.

2.3.6. Permeability measurements

The gas permeability measurements of polycyclic silicone membranes were carried out with a commercially available test cell (Gelman Science, Ann Arbor, MI) using pure H_2, N_2, O_2, CO_2 and CH_4 gases, at room temperature. The effective membrane area was 9.62 cm^2. The permeation rate was measured from 3 to 4 bar pressure difference with bubble flow meters. Special care was taken to avoid measuring each gas flux before reaching the steady state. Specially in case of slow gases, the measurements were regularly repeated during hours to be sure that the values were constant. The selectivity was obtained calculating the ratio between permeability values for different gases.

3. Results and discussion

3.1. Synthesis and characterization of silicone networks

The polycyclic silicone networks were obtained by means of platinum-catalyzed hydrosilylation reaction, which is a very important method to produce new silicon–carbon bonds. The reaction is an addition of hydridesilane to carbon–carbon multiple bonds, as follows:

$$\text{–Si–H} + \text{H}_2\text{C}=\text{CH–Si–} \xrightarrow{\text{Pt}} \underset{\beta\text{-adduct}}{\text{–Si–CH}_2\text{CH}_2\text{–Si–}}$$

$$+ \underset{\alpha\text{-adduct}}{\text{–Si–CH(CH}_3\text{)–Si–}}$$

This reaction has the advantage of taking place under mild conditions, and even at room temperature, and mainly to form no by-products, which prevents the shrinkage of the material. The hydrosilylation reaction generally gives a mixture of α- and β-adducts, the relative percentage of each is dependent on the monomers involved in the reaction, and normally the less hindered addition product dominates [14], i.e. generally the β-adduct is the major product.

Raman spectra (Fig. 2) were used for the molecular structural characterization of the PSM networks.

A sharp, from medium to weak intensity, band at about 1600 cm^{-1} for PSM_1, PSM_2, PSM_4 and PSM_5 samples was associated to the stretching mode of C=C vinyl group. For PSM_3, the band at 1584 cm^{-1} could be attributed to phenyl C=C stretching mode. PSM_1 and PSM_5 showed the presence of a very weak band characteristic of Si–H stretching at 2100 cm^{-1} [15]. These observations suggested the presence of unreacted functions, i.e. the functional groups, from network precursor units, were not totally incorporated in the network structure by the hydrosilylation reaction, mainly due to the increase of the steric hindrance around these groups in the course of the reaction. After gelation of the system, the mobility of the reagents and catalyst must be diminished, which also makes difficult the reaction.

In a polyfunctional system, even after annealing, considerable amount of unreacted, but reactive, groups still remain unable to cure, because of steric separation from the corresponding reactive group needed to effect cure; in this case, vinyl on D_4^V, TVS or TAS and SiH on D_4^H, TMDS or DSB. Kidera et al. [16] also describe the inequality in the reactivity of functional groups, i.e. when two or three groups of a molecule have already reacted, the reactivity of the last one should be lower due to steric hindrance, increasing the probability of the formation of linearly linked clusters.

The ratio between relative intensities of CH_2 bending (1405 cm^{-1}) and C=C vinyl stretching (1600 cm^{-1}) showed a higher hydrosilylation reaction yield for PSM_2 and PSM_3, the last one did not show the C=C band. Other characteristic scattering bands of the polycyclic silicone networks were at around: 2960 cm^{-1} (υ C–H), 1274 cm^{-1} (δ C–H), 1082 cm^{-1} (δ C–H phenyl), 760, 690 cm^{-1} (υ Si–C), 623

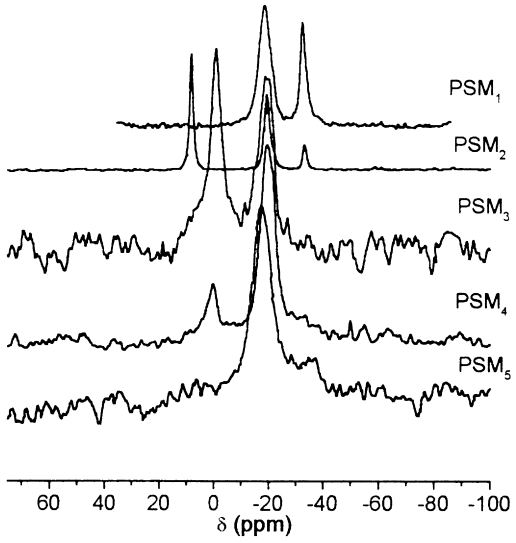

Fig. 3. ^{29}Si MAS NMR of PSM membranes.

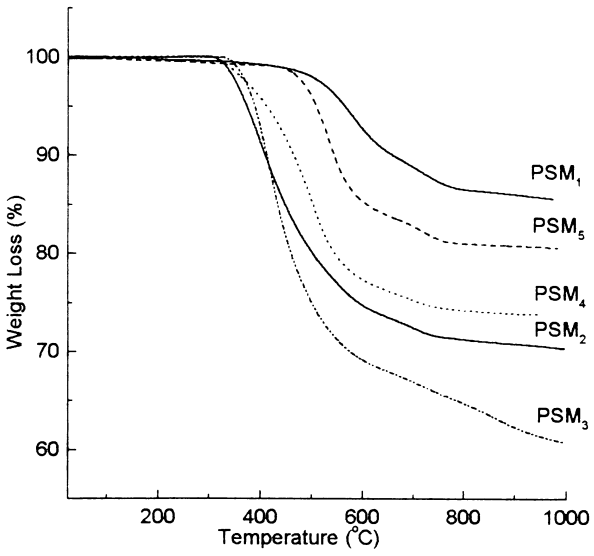

Fig. 4. TGA curves of polycyclic silicone membranes in argon atmosphere.

cm^{-1} (υ C–C phenyl) and 495 cm^{-1} (ring siloxane breathing mode, D_1 band) [15,17]. The last peak is similar to those found in inorganic-based silicate materials. According to Li and King [17], the red shift to lower wavenumbers of Si–O–Si Raman bands implies in the formation of a more open structure, which allows easier vibration to take place. Comparing the D_1 bands for the PSM samples, red shift was observed for PSM_2 and PSM_3, which is in agreement with the presence of difunctional monomers in their structures. For other membranes, the silicone network was obtained from two tetrafunctional monomers, which implies in a more strained structure. D_1 band, in the PSM_2 membrane, was split into two bands at 484 and 527 cm^{-1}, and the last was attributed to linear Si–O–Si groups from TMDS.

^{29}Si MAS NMR spectrum was also used for the molecular structural characterization of the membranes due to its great ability to distinguish between different structural siloxane units. The ^{29}Si MAS NMR spectra of polycyclic silicone networks are shown in Fig. 3. The ^{29}Si chemical shifts observed for siloxane units in the films are listed in Table 1.

All silicone network membranes showed a broad signal centered at −18 ppm, which is characteristic of the D units, $(C_2H_4)Si(CH_3)O_{2/2}$ [19], produced by hydrosilylation reaction of the cyclic monomers D_4^V and/or D_4^H. For PSM_1, PSM_2 and PSM_5 membranes, a signal at −32 ppm assigned to unreacted Si–H and/or Si–CH=CH_2 of the precursors, was also observed [19]. This result confirmed the presence of unreacted functional groups in these materials, as observed in the Raman analysis, as well as the absence of unreacted vinyl groups for PSM_3. The effective amount of Si–H and Si–CH=CH_2 involved in the formation of the polycyclic network, by hydrosilylation reaction, was calculated by the corresponding peak integrations and was 65, 90% and approximately 100% for PSM_1, PSM_2 and PSM_3, respectively. Reactions of 1, 2 or 3 functional groups give signals in the 0.08 to −1.98 ppm [20] and −24 to −10 ppm [21] range, for PSM_4 and PSM_5 films, respectively. So, the presence of a large signal in these regions makes the peak integration of individual units impossible to calculated.

Table 1
^{29}Si chemical shifts range for some siloxane units

Unit	Notation	δ (ppm) [18]
$MeEtSi(O–)_2$	D	−19 → −23.5
$MeViSi(O–)_2$	D^V	−32
$Me(H)Si(O–)_2$	D^H	−32 → −33
$Me_2EtSiO–$	M	6.1 → 9.8
$Me_2(H)SiO–$	M^H	−5.3 → −7.6
$Me_2EtSiPh$	–	−1
$Me_2(H)SiPh$	–	−17
$Et_{(x)}All_{(4-x)}Si$	–	+0.08 → −1.98
$Et_{(x)}Vi_{(4-x)}Si$	–	−10.7 → −30.3

3.2. Thermal–mechanical behavior

The thermogravimetric curves showed that all PSM membranes have good thermal stabilities, with initial temperatures of weight loss above 300°C, as can be seen in Fig. 4.

In systems with reduced chain mobility or rigid structures, such as poly(silphenylene–siloxane), Ikeda et al. [22] showed that the mechanism of decomposition is determined by bond energy factors. This process favors the cleavage of methyl groups, followed by the scission of silphenylene bonds. The Si–O bonds have higher bond energy and are cleaved at higher temperatures.

In PSM networks the mobility of Si–O–Si segments were drastically diminished by the polycyclic network formation, and the absence of end-block nucleophilic groups might contribute to thermal degradation processes with strong dependence of energy factors, like those in

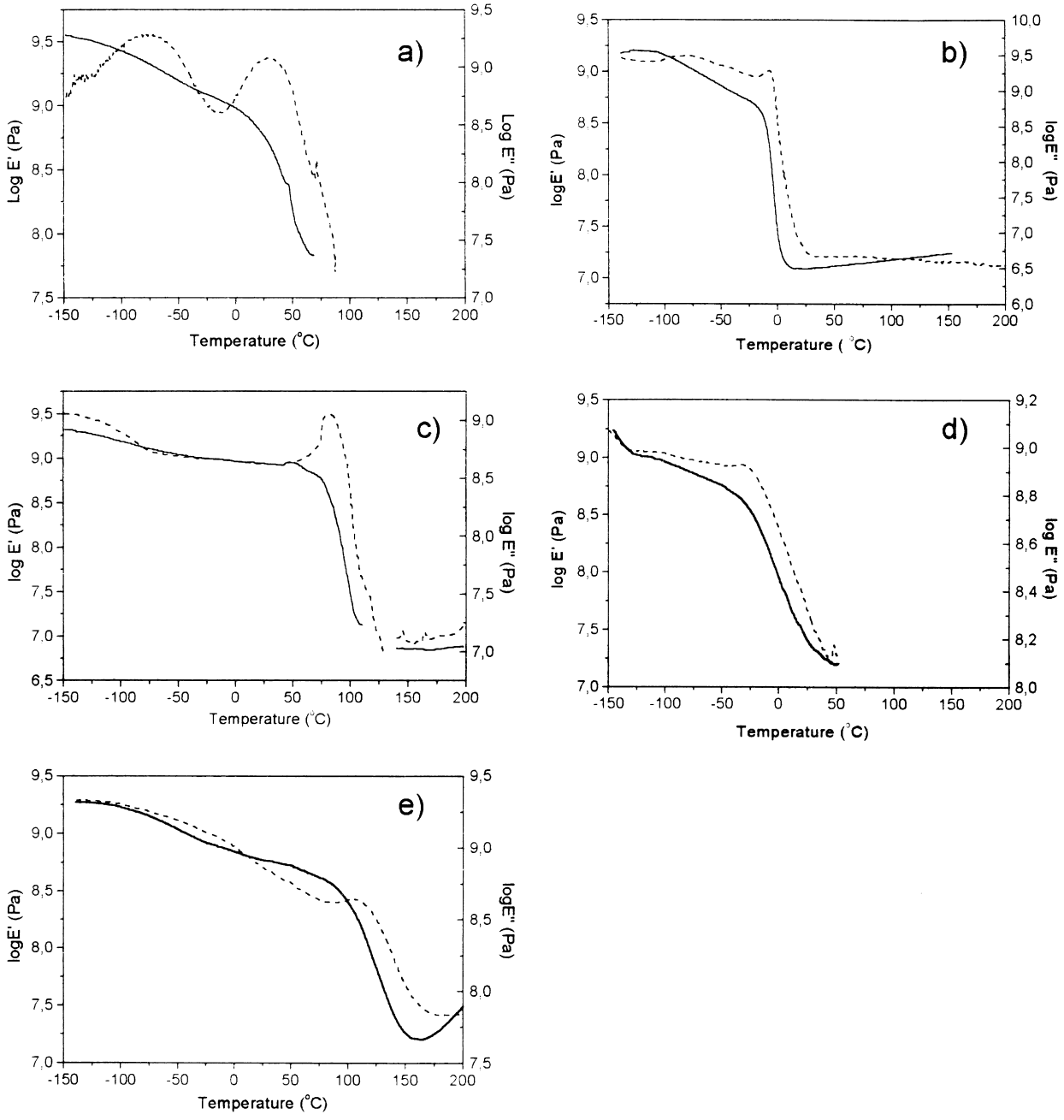

Fig. 5. Dynamic mechanical analysis of: (a) PSM_1; (b) PSM_2; (c) PSM_3; (d) PSM_4 and (e) PSM_5.

poly(silphenylene–siloxane) [8,22]. Michalczyk et al. [9] analyzed the thermal behavior of a silicone polycyclic system, analogous to PSM_1 membrane, and concluded that the first stage of weight loss was attributed to the cleavage of Si–C bonds of lateral organic groups. Li et al. [23] also described the thermal degradation of a 3D poly(methylsiloxane) by the same first stage of degradation process. Therefore, the first stage of weight loss, above 350°C, could be attributed to the cleavage of $Si–CH_3$, Si–vinyl and Si–phenyl groups, that have lower dissociation energies [9]. The second stage, above 570°C, was attributed to rearrangements of the network structure with the occurrence of redistribution reactions involving Si–H/Si–O and/or Si–C/Si–O bonds, followed by the mineralization of the material. This last process yields silicon oxycarbides, SiC_xO_{4-x} as the major product [18,24].

The storage modulus, E', and loss modulus, E'', curves of the PSM membranes are shown in Fig. 5.

Two transitions, the last and more intense being the glass transition, were observed in all cases. This profile, with two transitions, suggests the existence of phase segregation in the system. However, the cryogenic fracture surface of the films, observed by FESEM, did not show phase segregation, indicating that the films were homogenous at the resolution

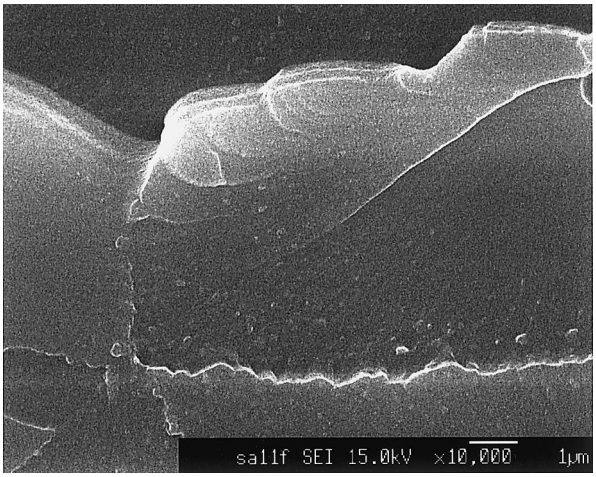

Fig. 6. FESEM micrograph of cryogenic surface fracture of PSM_1 membrane.

limit of the equipment. All the PSM membrane films showed similar patterns, with homogeneous and featureless fracture surfaces, as can be seen for PSM_1 in Fig. 6.

On the other hand, the transition width reflects the number of relaxation modes associated to this process [25,26]. The presence of segments with different conformations, mobilities or chemical environments, gives rise to different relaxation times, and consequently broad transitions. Thus, the profiles observed for PSM membranes suggest a large distribution of micro-environments that may stem from different degrees of connectivity between cycles. Narrower glass transitions were observed for PSM_2 and PSM_3 membranes, in which a high percentage of functional groups participated of the hydrosilylation reaction (Figs. 5b and c). These results are in agreement with the ^{29}Si MAS NMR and Raman analyses, and suggest that the siloxane cycles must be connected by variable numbers of functions, which give rise to regions with different degrees of connectivity and therefore, different mobilities.

3.3. Force atomic microscopy

It is often observed that synthetic polymeric membranes have patterns on the surface, similar to the observed on surfaces of biological membranes. The patterned surfaces are more advantageous for the material transport due to their larger surface area. Fig. 7 (a, b, c) displays typical $70 \times 70\ \mu m^2$ AFM images of the top surface of PSM_1, PSM_2 and PSM_3 membranes, respectively. These images indicates some differences in the surface morphologies, characterized by the presence of nodular structures, mainly in PSM_1, while PSM_3 surface reveals the presence of depression regions, which are not present in the other membranes. PSM_1 also shows in the $70 \times 70\ \mu m^2$ scan size, the highest root mean square value of z values (RMS) while PSM_3 presents the highest difference between the mean height of the nodules and the mean depth of the valleys (R_z). It is reported that the mean roughness (R_a) of the membrane (measured by AFM) was directly proportional to the permeability of gases, with some exceptions [27]. The PSM dense membranes did not show this relationship. The flat regions among the nodular or depression structures are shown in the corresponding $5 \times 5\ \mu m^2$ scan size displays, Fig. 7 (d, e, f). The surface roughness measurements were found to be dependent on the surface area being scanned. These images reveal that PSM_1 and PSM_2 have sponge-like structures.

3.4. Small angle X-ray acattering

The morphology of the silicone polycyclic membranes was also studied by SAXS. This technique measures the angular dependence of the intensity scattered by a sample with electron density heterogeneities ($\Delta\rho$) [28]. If an electron density contrast ($\Delta\rho$) in the system exists [29], the small-angle X-ray scattering must occur, with scattering intensity proportional to $\Delta\rho$.

X-ray scattering was not observed for PSM_2 and PSM_3, which suggests the absence of scattering entities, or if they exist, their dimensions are out of the detection range of the SAXS instrumentation. Scattering profiles characteristic of polydisperse systems were observed for PSM_1, PSM_4 and PSM_5. The more evident structural heterogeneities observed in DMA, which were attributed to regions with different degrees of connectivity between siloxane cycles, can lead to different electron densities, and can be the origin of the observed scattering. These materials grow as 3D networks, and they can adopt several conformations, and therefore they would have regions with different electron densities. Similar behavior was recently described by Urayama et al. [30] in swollen PDMS networks, where the scattering profile suggested the presence of spatial inhomogeneity frozen in the network. This inhomogeneity was attributed to a non-uniform distribution of the crosslink centers leading to the formation of regions with connectivity fluctuations.

The scattered intensity from isolated aggregates, at very small angles can be analyzed by Guinier's equation (1), leading to the calculation of the radii of gyration (R_g):

$$I(q) = (\Delta\rho)^2 V^2 \exp(-R_g^2 q^2/3) \quad (1)$$

In this equation, $I(q)$ represents the intensity, V the scattering center volume and q the scattering vector. The SAXS profiles for PSM membranes did not show a clear Guinier behavior. This indicates that the nanostructure of these materials cannot be described as a system of isolated particles and/or pores. Further structural information could be obtained in the higher angle (power law) region.

Fractal geometry has been used as an important concept to characterize amorphous materials [31]. The fractal dimension D is obtained from the analysis of the power-law region ($10^{-2} < q < 10^{-1}$ Å^{-1}). In this region, the scattering profiles do not depend on the shape of the scattering units. The bi-logarithmic plots of the intensity as a function of q revealed that the polycyclic silicone networks

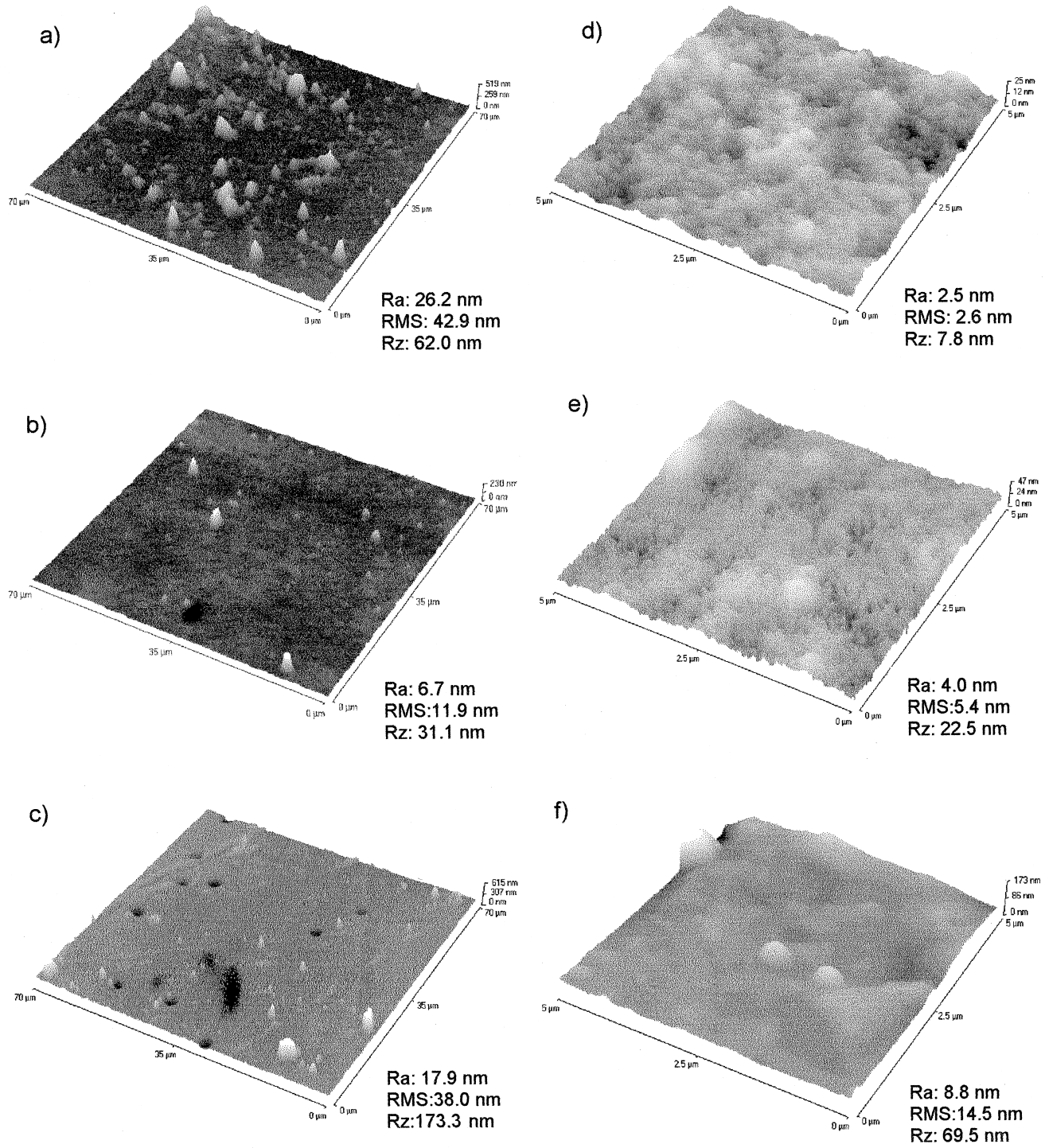

Fig. 7. AFM images of the top surface of the polycyclic silicone membranes ($70 \times 70\ \mu m^2$) : (a) PSM_1; (b) PSM_2 and (c) PSM_3 ($5 \times 5\ \mu m^2$) : (d) PSM_1 (e) PSM_2 and (f) PSM_3. The vertical scales are greatly exaggerated to display clearly the spatial amplitude in the *z*-direction.

membranes are mass fractals, with D values of 1.44, 1.98 and 2.61 for PSM_1, PSM_4 and PSM_5, respectively. Mass fractals resemble polymer-like structures as opposed to colloid-like objects (uniformly dense). According to Martin et al. [32] as the fractal dimension decreases, the structures appear sparser, more open, until they reach $D = 1$, where the object becomes linear, while the increase in D values suggests a more compact network. The PSM_1 network showed the lowest value of D, which implies in a more open structure probably due to great steric hindrance during the network formation. Comparing PSM_4 and PSM_5 membranes, the former showed the lower D value, which could be explained by the greater percentage of unreacted functional groups, as observed in Raman spectra.

Table 2
Gas permeabilities of PSM, PDMS and some organic membranes used in gas separation processes

Gases	P^a					
	PSM_1	PSM_2	PSM_3	Cellulose acetate [10]	Bisphenol-A polysulfone [10]	PDMS [10]
O_2	70 ± 2	179 ± 2	31 ± 1	0.15	0.19	781
N_2	15.0 ± 0,8	61.0 ± 1,5	8.0 ± 0,4	0.82	1.2	351
CO_2	423 ± 6	982 ± 3	132.0 ± 1,4	0.15	0.18	4550
CH_4	43.0 ± 1,3	2010 ± 1,4	11.0 ± 0,1	4.75	4.6	1430
H_2	238 ± 2	313.0 ± 1,4	127 ± 3	–	–	–

[a] P (barres) $= 10^{-10}$ (cm^3 (NTP) cm/cm^2s cmHg).

3.5. Permeability measurements

The permeabilities of H_2, N_2, O_2, CO_2 and CH_4 through PSM_1, PSM_2 and PSM_3 silicone membranes, are summarized in Table 2, and the selectivity values are shown in Table 3.

The measurements were performed with a bubble flow meter as used by Sforça et al. [33], and the results were similar to those obtained by a system using vacuum in the permeate side and variable pressures on the feed side, particularly for N_2. However, CO_2 permeability was greater in the former system.

Analyzing the permeability values obtained for PSM membranes and comparing with those of PDMS, a decrease in the permeability was observed. The high permeability of PDMS has been attributed to its large free volume, which may be due to the great flexibility of its siloxane links [10].

Gas transport in polymers is generally referred to as a solution/diffusion process, the permeability coefficient (P) being the product of the diffusion (D) and the solubility (S) coefficients [34]:

$$P = D \times S$$

The diffusion coefficients for small molecules in polymers are strongly affected by chain-packing density, and therefore by the free volume amount [35]. High chain flexibility causes large diffusion coefficients and low apparent activation energies for diffusion. PSM membranes have a composition rich in siloxane groups. However, these materials have a high connection density between cycles, which causes a great decrease in the chain flexibility and in the free volume.

The permeability values observed for PSM membranes reflect the differences in their structures, as the different monomers give rise to materials with variable stiffness. The glass transition temperatures, observed by DMA, were 50, −8 and 82°C, respectively for PSM_1, PSM_2 and PSM_3, which are in agreement with the highest permeability value for the PSM_2 membrane, while the PSM_3 sample presented the lowest.

It can also be seen that the selectivity values for PSM membranes were higher than those for the PDMS-based membranes, which is in agreement with the inverse relationship usually observed between permeability and selectivity for common gases [34]. Comparing the permeability and selectivity values of PSM membranes with those of organic membranes [10], it can be noticed that the former present considerable advantages for the use in gas separation processes. The permeability values are greater than those of organic membranes and the selectivity values are of the same order of magnitude in some cases.

4. Conclusions

Polycyclic silicone membranes were obtained by hydrosilylation reactions, from tetrafunctional siloxane cycles, with good thermal stability and mechanical properties, and a wide distribution of structural heterogeneities, as a consequence of different degrees of connectivity between the cycles. Morphological analyses showed homogeneous and nonporous materials with roughness surfaces. These membranes showed lower permeability and higher selectivity coefficients than the membranes obtained from linear PDMS, with potential application in gas separation processes.

Acknowledgements

The authors would like to thank to FAPESP for the

Table 3
Selectivity values of PSM, PDMS and some organic membranes used in gas separation processes

Selectivity	Membranes					
	PSM_1	PSM_2	PSM_3	Cellulose acetate [10]	Bisphenol-A polysulfone [10]	PDMS [10]
O_2/N_2	4.6 ± 0.1	2.9 ± 0.1	3.9 ± 0.1	5.5	6.3	2.2
CO_2/CH_4	9.2 ± 0.2	4.9 ± 0.1	12.0 ± 1.5	32	26	3.2

financial support (Process numbers 95/03636-3 and 97/06136-4) and to LNLS for the SAXS measurements.

References

[1] Mark JE. Silicon based polymer science, a comprehensive resource. In: Ziegler JM, Fordon FW, editors. Adv Chem Ser 224, Washington DC: American Chemical Society, 1990 (chap 2).
[2] Polymer handbook. In: Bramdrup J, Immergut EH, editors. Polymer handbook, New York: Wiley, 1975.
[3] Dvornic PR, Lenz RW. Macromolecules 1992;25:3769.
[4] Dvornic PR, Lenz RW. In: Dvornic PR, Lenz RW, editors. High temperature siloxane elastomers, New York: Hüthig and Wepf Verlag Basel, 1990 (chap 2).
[5] Clarson SJ. In: Clarson SJ, Semlyen JA, editors. Siloxane polymers, Englewood Cliffs, NJ: Prentice Hall, 1993 (chap 5).
[6] Dvornic PR, Lenz RW. Polymer 1983;24:763.
[7] Thomas TH, Kendrick TC. J Polym Sci Part A2 1969;07:537.
[8] Werlang MM, Yoshida IVP, Araújo MA. J Inorg Organomet Polym 1995;5:75.
[9] Michalczyk MJ, Farneth WE, Vega AJ. Chem Mater 1993;5:1687.
[10] Stern SA. J Membr Sci 1994;94:1.
[11] Robenson M, Burgone WF, Langsam M, Savoca AC, Tien CF. Polymer 1994;35:4970.
[12] Pittman CU, Patterson WJ, Macmanus SP. J Polym Sci Polym Chem Ed 1976;14:1715.
[13] O'Brien S, Fishwick M, McDermott B, Wallbridge MGH, Wright GA. Inorganic Syntheses 1971;13:73.
[14] Kendrick TC, Parbhoo B, White JW. In: Patai S, Rappoport Z, editors. The chemistry of organic silicon compounds, New York: Wiley, 1989 (part 2, chap 21).
[15] Calzaferri G, Marcolli C, Imhof R, Tornroos KW. J Chem Soc Dalton Trans 1996;15:3313.
[16] Kidera A, Higashira T, Ikeda Y, Urayama K, Kohjiya S. Polym Bull 1997;38:461.
[17] Li X, King TA. J Non-Cryst Solids 1996;204:235.
[18] Belot V, Corriu RJP, Leclercq D, Mutin PH, Vioux A. J Polym Sci: Part A Polym Chem 1992;30:613.
[19] Harris RK, Kimber BJ, Wood MD. J Organometal Chem 1976;116:291.
[20] Delmulle L, Van Der Kelen GP. J Molec Struct 1980;66:315.
[21] Delmulle L, Van Der Kelen GP. J Molec Struct 1980;66:309.
[22] Ikeda M, Nakamura T, Nagase Y, Ikeda K, Sekine Y. J Polym Sci Polym Chem Ed 1981;19:2595.
[23] Li D, Huang ST. J Appl Polym Sci 1992;44:1979.
[24] Radovanovic E, Gozzi MF, Gonçalves MC, Yoshida IVP. J Non-Cryst Solids 1999;248:37.
[25] Wetton RE. In: Dawkins JV, editor. Developments in polymer characterization, London: Elsevier Applied Science, 1986 (chap 5).
[26] Roberts GE, White EFT. In: Haward RN, editor. The physics of glassy polymers, First ed. London: Elsevier Applied Science, 1973 (chap 3).
[27] Khulbe KC, Matsura T. Polymer 2000;41:1917.
[28] Ramirez-del-Solar M, Esquivias L, Craievich AF, Zarzycki J. J Non-Cryst Solids. 147 and 1992;148:206.
[29] Breiner JM, Mark JE. Polymer 1999;39:5483.
[30] Urayama K, Kawamura T, Hirata Y, Kohjiya S. Polymer 1998;39:3827.
[31] McCarthy DW, Mark JE, Schaefer DW. J Polym Sci: Part B Polym Phys 1998;36:1167.
[32] Martin JE, Hurd AL. J Appl Cryst 1997;20:61.
[33] Sforça ML, Yoshida IVP, Nunes SP. J Membr Sci 1999;159:197.
[34] Petropoulos JH. J Membr Sci 1990;53:229.
[35] Wang Z, Chen T, Xu J. J Appl Polym Sci 1997;64:1725.